N90-28244

On the Dynamic and Thermodynamic Structures of Marine Stratocumulus

Mark J. Laufersweiler and Hampton N. Shirer
Department of Meteorology
The Pennsylvania State University
University Park, PA 16802

Latent heating effects on stratocumulus circulations have been studied successfully with a nine-coefficient spectral model of two-dimensional shallow Boussinesq convection (Laufersweiler and Shirer, 1989: JAS, 1133-1153). Further, more realistic investigations are being performed currently with a larger, 18-coefficient spectral model, in which the effects of cloud top radiational cooling and in-cloud radiational heating are also being represented. Because assuming a rigid lid at the inversion base may have affected previous results significantly, we have raised the domain top to include the lower portion of the capping inversion. As in the previous model, a uniform cloud base is assumed and latent heating effects are included implicitly such that the motions in the sub- and above-cloud regions are dry adiabatic and the motions in the cloud region are moist adiabatic. The effects of forcing by radiational heating profiles that are tied to the cloud layer, such as the one used by Nicholls (1984: QJRMS, 783-820), will be investigated, as will profiles measured during the FIRE experiment.

One concern of using truncated spectral models is that the phenomena are so poorly represented that they can change dramatically as the number of spectral coefficients is increased. The efficacy of the nine-coefficient model results is checked by examining the steady state solutions of the 18-coefficient model for parameter values used by Laufersweiler and Shirer (1989), which corresponds to the case of a moderately deep cloud and no capping inversion (Fig. 1). Here, the horizontally asymmetric circulation patterns that have narrow downdraft areas and broad updraft areas are virtually the same as those found in the smaller spectral model (Fig. 1b). Also captured in the case of weaker heating is an elevated circulation centered at cloud base (Fig. 1a). Thus, the results of the smaller model are substantiated.

Since one of the goals of studying the new model is to represent a more realistic domain, the second test of the model is to investigate whether the steady solutions are suppressed in the case of an inversion with no cloud. The capping inversion should limit the convective circulations, but we do not force this to happen with the imposition of a rigid lid at the inversion base. Figure 2 shows the steady solutions for the case of a relatively strong inversion of 10 °C/km that begins at a height of $0.8z_t$, as indicated by the tic. For the case when the value of the Rayleigh number is near its critical value (Fig. 2a), the circulations are weak and located in the sub-inversion region of the domain. For a higher value of the Rayleigh number (Fig. 2b), the circulation has intensified but is still restricted to the sub-inversion region; importantly, the updrafts only penetrate into the inversion by a small amount. Thus, the model is correctly representing the effects of an inversion by properly suppressing the convection.

Figures 3 and 4 are the first investigations into the performance of the model when both the cloud and an inversion are represented. Figure 3 shows the steady solutions for a weak inversion having a value of 2 °C/km and Fig. 4 shows the steady solutions for a fairly strong inversion having a value of 10 °C/km. The higher value of the inversion strength, although large, is still on the order of 1/2 of the values of the inversion strength that were measured during FIRE, typically around 18 to 20 °C/km. By comparing the figures, we observe that the intensity of the circulation patterns for the weaker inversion is stronger than that for the stronger inversion; however, we are concerned that for higher values of the Rayleigh number, the circulations penetrate too deeply into the inversion. This result may be due to the fact that the latent heating, as represented in this model, is warming the flow far more than that found in the actual boundary layer. Possibly, inclusion of radiative forcing will compensate for this effect.

The research for this work was supported in part by the National Science Foundation through Grant ATM-8619854 and by the Office of Naval Research through Contract N000014-86-K-06880.

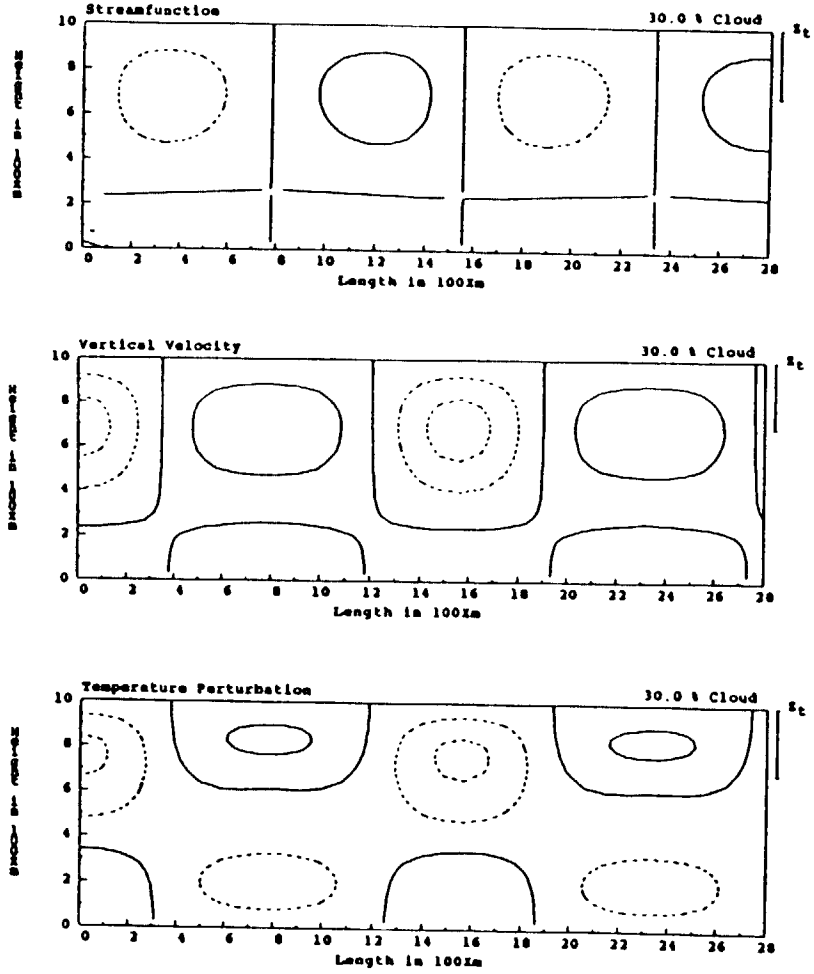

(a)

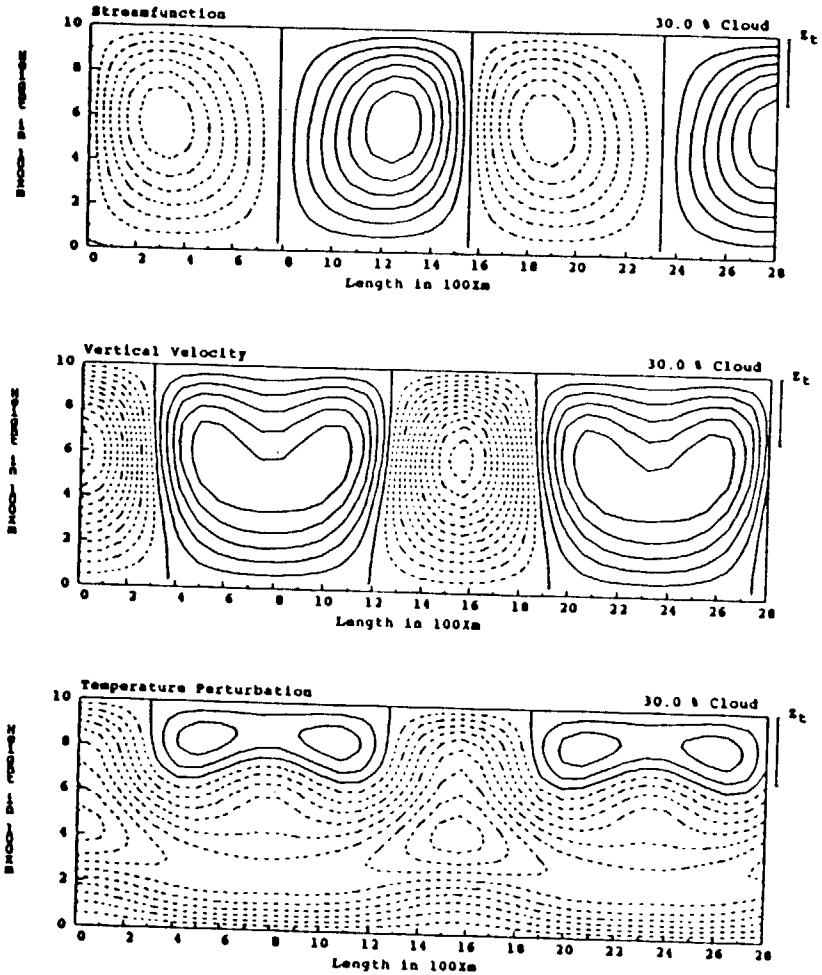

(b)

Figure 1. The steady state dimensionless streamfunction ψ^*, vertical velocity w^* and temperature perturbation T^* for a cloud covering 30% of the domain for $Ra - Ra_c = 4.9$ (a) and 84.9 (b) for a non-inversion case corresponding to the nine-coefficient model. Here the cloud region is indicated by the vertical line to the right of each figure. The dashed lines represent negative values of the fields. The contour intervals are 1 for the streamfunction, 1 for the vertical velocity and 15 for the temperature perturbation.

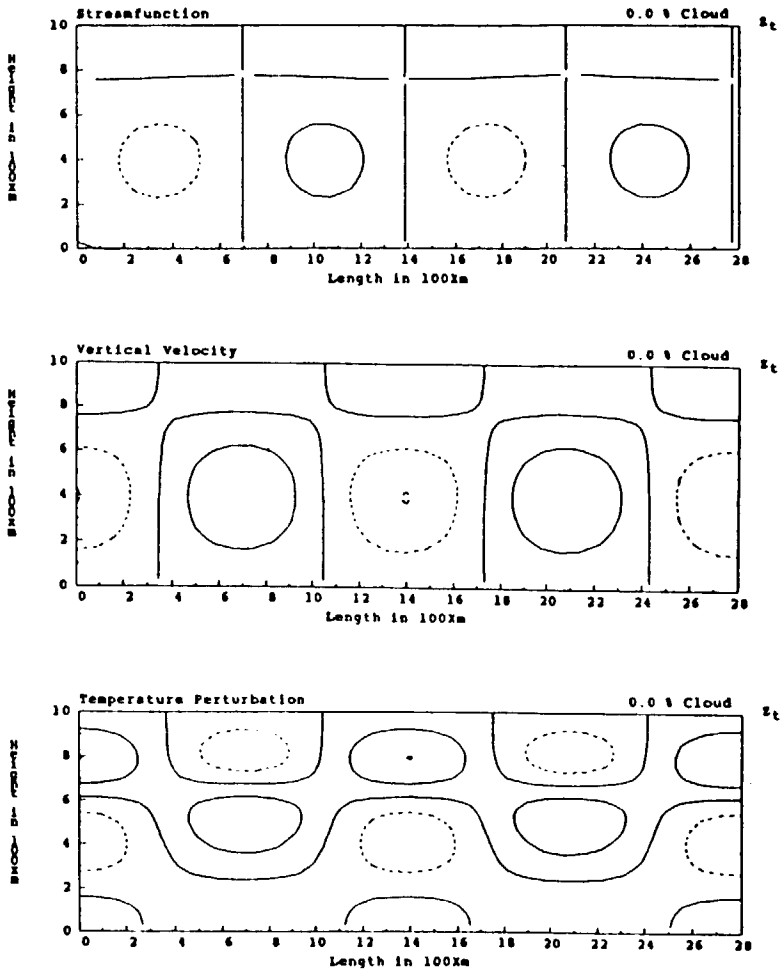

(a)

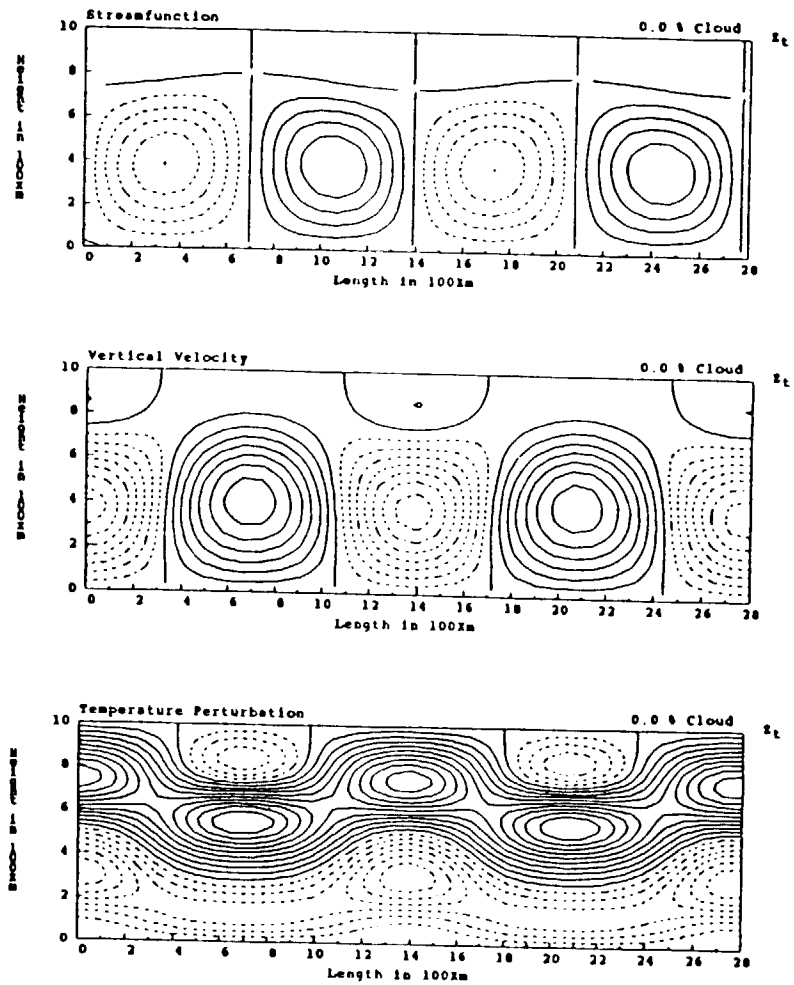

(b)

Figure 2. The steady state dimensionless streamfunction ψ^*, vertical velocity w^* and temperature perturbation T^* for a cloud-free case with an inversion based at $z = 0.7z_t$ and having the value 10 °C/km for $Ra - Ra_c = 7.8$ (a) and 97.8 (b). On the right of each figure, the base of the inversion is shown by the tic. The dashed lines represent negative values of the fields. The contour intervals are the same as in Fig. 1.

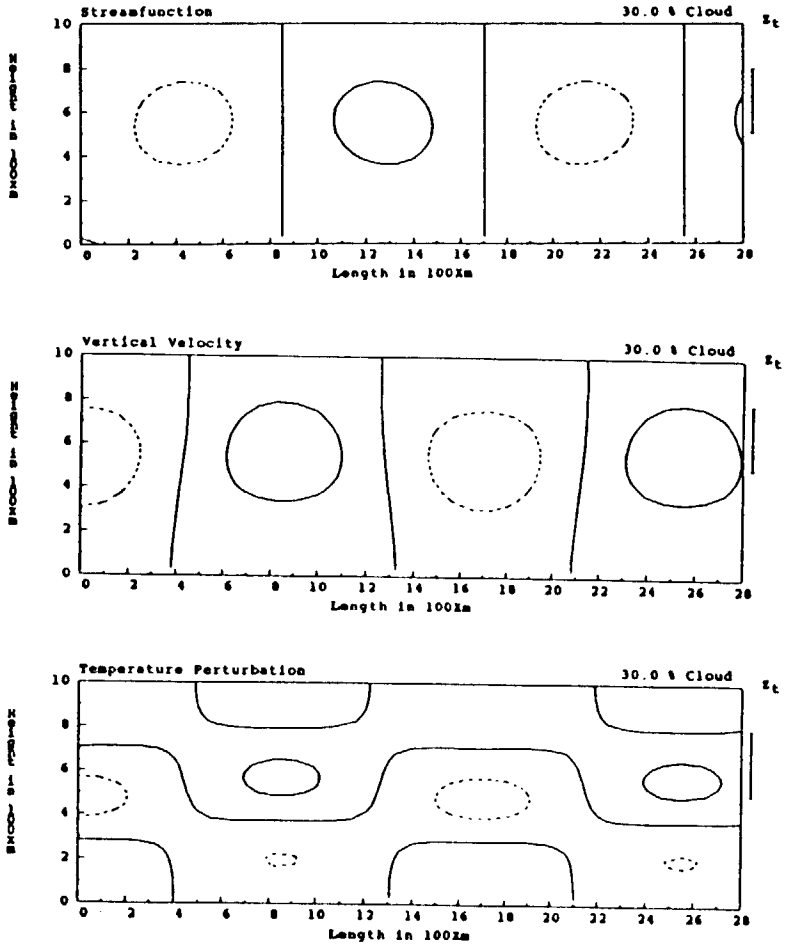

(a)

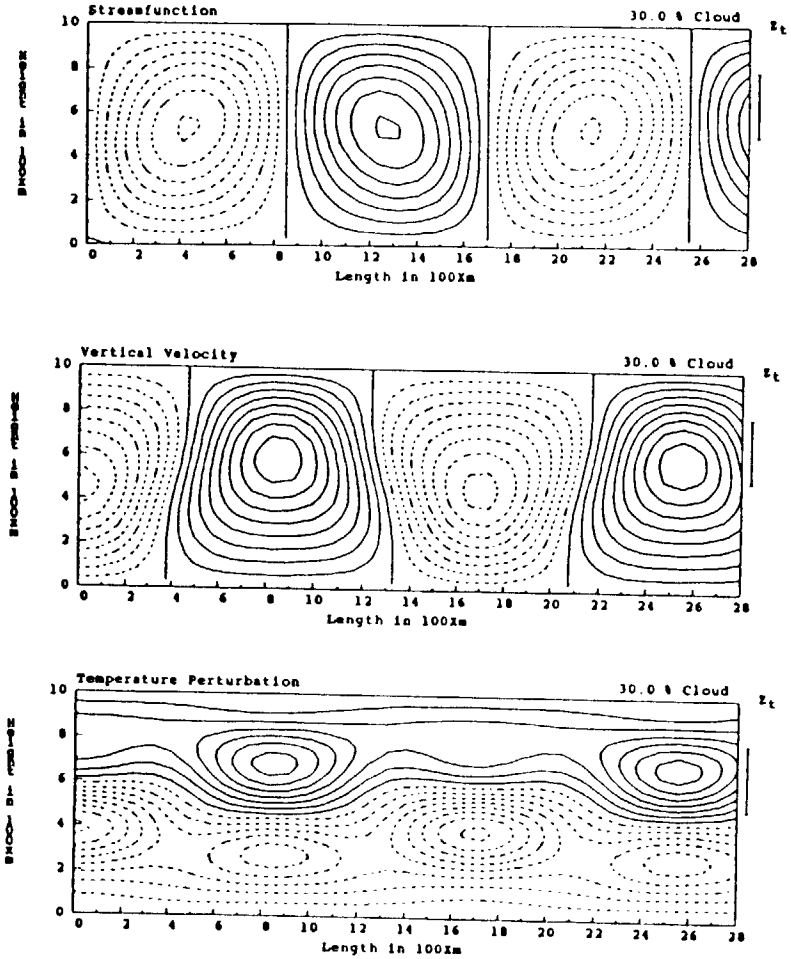

(b)

Figure 3. The steady state dimensionless streamfunction ψ^*, vertical velocity w^* and temperature perturbation T^* for a cloud covering 30% of the domain with an inversion based at $z = 0.8z_t$ having the value 2 °C/km for Ra - Ra_c = 4.9 (a) and 74.9 (b). On the right of each figure, the cloud region is indicated by the vertical line, with the inversion base at cloud top. The dashed lines represent negative values of the fields. The contour intervals are the same as in Fig. 1.

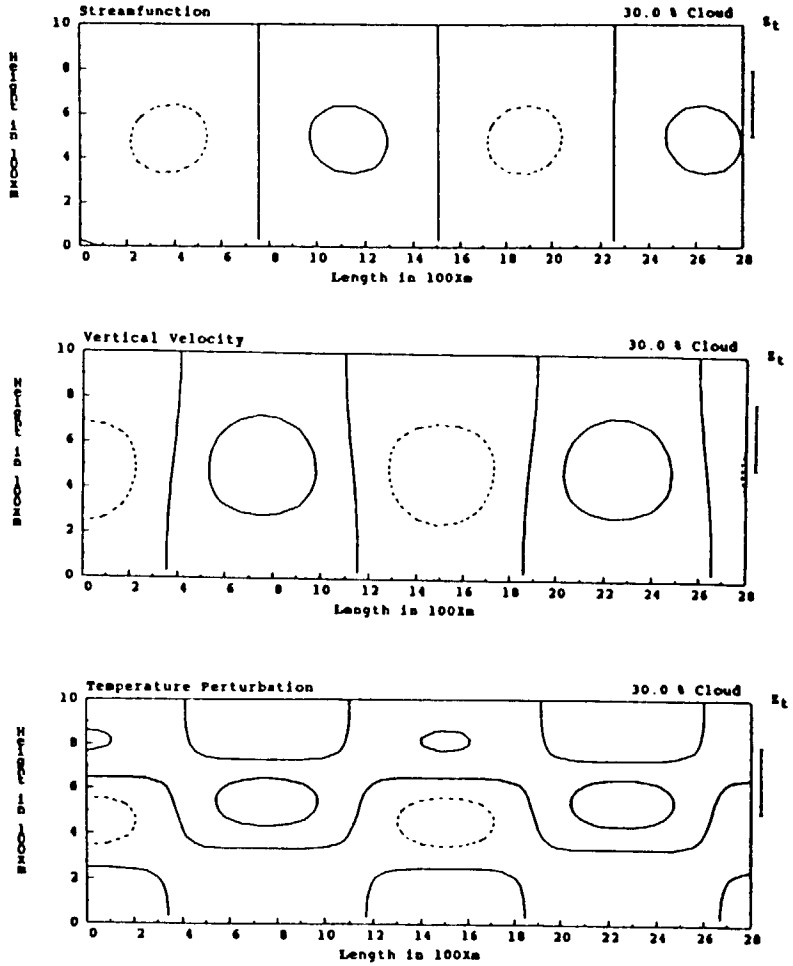

(a)

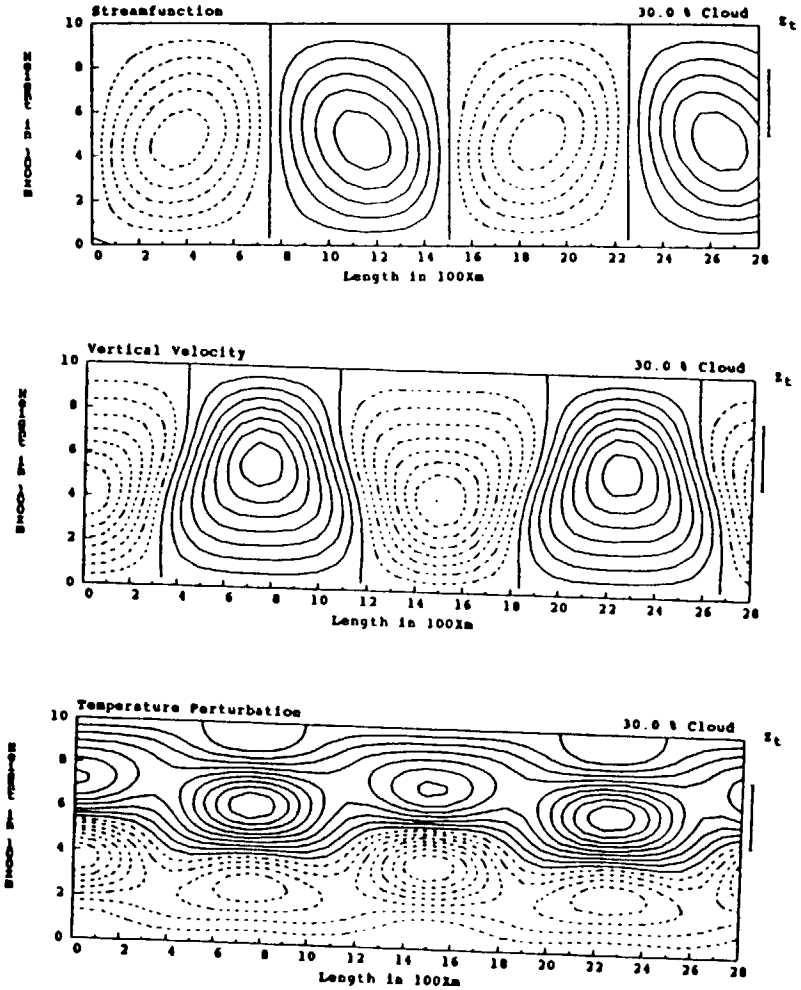

(b)

Figure 4. The steady state dimensionless streamfunction ψ^*, vertical velocity w^* and temperature perturbation T^* for a cloud covering 30% of the domain with an inversion based at $z = 0.8z_t$ having the value 10 °C/km for $Ra - Ra_c = 13.7$ (a) and 56.3 (b). On the right of each figure, the cloud region is indicated by the vertical line, with the inversion base at cloud top. The dashed lines represent negative values of the fields. The contour intervals are the same as in Fig. 1.